

Spherical collapse model with shear and angular momentum in dark energy cosmologies

A. Del Popolo^{1,2*}, F. Pace³, J. A. S. Lima²

¹ *Astronomy Department, University of Catania, Italy*

² *Departamento de Astronomia, Universidade de São Paulo, Rua do Matão 1226, 05508-900, São Paulo, SP, Brazil*

³ *Institute of Cosmology and Gravitation, University of Portsmouth, Dennis Sciama Building, Portsmouth, PO1 3FX, U.K.*

Received August 14, 2018; accepted ?

ABSTRACT

We study, for the first time, how shear and angular momentum modify typical parameters of the spherical collapse model, in dark energy dominated universes. In particular, we study the linear density threshold for collapse δ_c and the virial overdensity Δ_v , for several dark-energy models and its influence on the cumulative mass function. The equations of the spherical collapse are those obtained in Pace et al. (2010), who used the fully nonlinear differential equation for the evolution of the density contrast derived from Newtonian hydrodynamics, and assumed that dark energy is present only at the background level. With the introduction of the shear and rotation terms, the parameters of the spherical collapse model are now mass-dependant. The results of the paper show, as expected, that the new terms considered in the spherical collapse model oppose the collapse of perturbations on galactic scale giving rise to higher values of the linear overdensity parameter with respect to the non-rotating case. We find a similar effect also for the virial overdensity parameter. For what concerns the mass function, we find that its high mass tail is suppressed, while the low mass tail is slightly affected except in some cases, e.g. the Chaplygin gas case.

Key words: cosmology: theory - dark energy - methods: analytical

1 INTRODUCTION

Till a decade ago, Universe was considered composed mainly by dark matter (DM) and characterized by a decelerating expansion. An important and surprising result coming from observational cosmology is the fact that high redshift supernovae are less bright than expectations (Riess et al. 1998; Perlmutter et al. 1999; Tonry et al. 2003). This finding has been interpreted as an acceleration in the expansion of the universe and that this acceleration is recent (Riess et al. 1998; Perlmutter et al. 1999; Knop et al. 2003; Riess et al. 2004; Astier et al. 2006). This result has been confirmed by independent observations: the baryon acoustic oscillation (Tegmark et al. 2004; Eisenstein et al. 2005; Percival et al. 2010), the galaxy-galaxy correlation function, giving important infos on the spatial distribution of large-scale structure (Tegmark et al. 2004; Cole et al. 2005), the angular spectrum of the CMBR temperature fluctuations (Komatsu et al. 2011; Larson et al. 2011), the Integrated Sachs-Wolfe (ISW) effect (Ho et al. 2008), globular clusters (Krauss & Chaboyer 2003; Dotter et al. 2011), old high redshift galaxies (Alcaniz et al. 2003, 2005), and galaxy clusters (Haiman et al. 2001; Allen et al. 2004, 2008; Basilakos et al. 2010) and weak lensing (Hoekstra et al. 2006; Jarvis et al. 2006). The quoted accelerated expansion cannot be obtained in uni-

verses containing just matter homogeneously and isotropically distributed, while it can be obtained if the low- z universe is filled in with a fluid with negative pressure, the so called *dark energy* (DE), with equation-of state-parameter $w < -1/3$. It is possible to have accelerated universes without dark energy if one discards the homogeneity hypothesis on large scales (e.g., Lemaitre-Tolman-Bondi (LTB) universes), using the back-reaction approach to dark energy (Kolb et al. 2006), gravitationally induced particle creation (Lima et al. 2009, 2010) or even modified models of gravity, like the $f(R)$ models (Amendola et al. 2007), $f(T)$ models (Bengochea & Ferraro 2009), or the brane models (Deffayet 2001).

The nature of dark energy is not understood to date, and this explains why in the past decade a large number of models for the origin and time evolution of DE have been proposed. In the Λ CDM model the DE is connected to the energy of vacuum (cosmological constant) and the equation of state of DE, in this case, is simply $w = -1$. An extension of this model is obtained considering a scalar field with no or weak interaction with the matter component (quintessence models), and also phantom models, K-essence, or alternatively Chaplygin gas and Casimir effect.

Cosmologists generally believe that structures in the universe grew via gravitational instability through the growth and collapse of primeval density perturbations originated in an inflationary phase of early Universe from quantum, Gaussian distributed, fluctuations

* adelpopolo@astro.iag.usp.br

(Guth & Pi 1982; Hawking 1982; Starobinsky 1982; Bardeen et al. 1986).

The presence of DE changes the rate of formation and growth of collapsed structures and large-scale structure, and consequently the distribution in size, in time and space of galaxies, quasars, supernovae, since they reside in collapsed structures. Moreover, DE, increasing the expansion rate, slows down the collapse of overdense structure and its space-time fluctuations (if DE is not the cosmological constant) will give rise to DE haloes (Creminelli et al. 2010) which will influence dark halos formation.

In principle, all the statistical information concerning the distribution of the dark matter and DE is contained in the probability distribution functions (PDFs) for the velocity, \vec{v} , and mass density fluctuation fields, δ . The determination of the final moments of the quoted distribution from the starting ones require to know the exact dynamics ruling the evolution of the underlying field. Unfortunately the exact solution to the dynamical equations is known only in the linear regime of evolution of the quoted fields, and only approximate solutions are known for non-linear stages. A popular analytical approach to study the non-linear evolution of perturbations of DM and DE is the spherical collapse model (SCM) introduced in the seminal paper of Gunn & Gott (1972) extended and improved in several following papers (Fillmore & Goldreich 1984; Bertschinger 1985; Hoffman & Shaham 1985; Ryden & Gunn 1987; Avila-Reese et al. 1998; Subramanian et al. 2000; Ascasibar et al. 2004; Williams et al. 2004). Some papers (Hoffman 1986, 1989; Zaroubi & Hoffman 1993) addressed the issue of the role of velocity shear in the gravitational collapse.

The model describes how a spherical symmetric overdensity¹ decouples from the Hubble flow, slows down, turns around and collapse. In the model the overdensity is divided into bound mass, each one expanding with the Hubble flow from an initial comoving radius x_i to a maximum one x_m (usually named turn-around radius, x_{ta}), and then collapse. Non-linear processes convert the kinetic energy of collapse into random motions, giving rise to a “virialized” structure.

The SCM proposed by Gunn & Gott (1972) does not contain non-radial motions and angular momentum. The way to introduce angular momentum in the SCM, and its consequences, were studied in several papers (Ryden & Gunn 1987; Gurevich & Zybin 1988a,b; White & Zaritsky 1992; Sikivie et al. 1997; Avila-Reese et al. 1998; Nusser 2001; Hiotelis 2002; Le Delliou & Henriksen 2003; Ascasibar et al. 2004; Williams et al. 2004; Zukin & Bertschinger 2010).

Ryden & Gunn (1987) were the first to relax the assumption of purely radial self-similar collapse by including non-radial motions arising from secondary perturbations in the halo. Williams et al. (2004) used the same model to show how angular momentum flattens the inner profile of haloes. The effect of non-radial motions on the mass profile in a SCM was studied by Gurevich & Zybin (1988a,b).

White & Zaritsky (1992) applied a torque to particles in the shells during the initial expansion phase, and in order to preserve the spherical symmetry, assumed that the different particles acquire the same angular momentum but in independent randomly oriented directions. In Nusser (2001), particles acquire an angular momentum at turn around, while before they move on radial or-

bits. Again, in order spherical symmetry is preserved and the angular momentum of each particle is conserved, particles have angular momenta distributed in random directions such that the mean angular momentum at any point in space is zero. Moreover, angular momentum is $\propto \sqrt{GM(< r_*)}r_*^2$ per unit mass (White & Zaritsky 1992; Sikivie et al. 1997), so no additional physical scale is introduced. Other studies (Hiotelis 2002; Le Delliou & Henriksen 2003; Ascasibar et al. 2004) introduced angular momentum in the SCM in a similar way of the previous cited authors, and studied the structure of DM density profiles, reaching similar conclusions to that of Williams et al. (2004).

The SCM in the framework of dark energy cosmologies was studied by Mota & van de Bruck (2004); Abramo et al. (2007); Basilakos et al. (2010); Pace et al. (2010). In particular in Pace et al. (2010) were derived the equations for the SCM under the assumption that only DM can form clumps and that DE is present as a background fluid (see also Fosalba & Gaztañaga 1998; Ohta et al. 2003, 2004; Mota & van de Bruck 2004; Abramo et al. 2007). The evolution of the overdensity δ is given by (Pace et al. 2010, 2012):

$$\ddot{\delta} + 2H\dot{\delta} - \frac{4}{3}\frac{\dot{\delta}^2}{1+\delta} - 4\pi G\bar{\rho}\delta(1+\delta) - (1+\delta)(\sigma^2 - \omega^2) = 0. \quad (1)$$

the shear term $\sigma^2 = \sigma_{ij}\sigma^{ij}$ and the rotation term $\omega^2 = \omega_{ij}\omega^{ij}$ are connected to the shear tensor, which is a symmetric traceless tensor, while the rotation is antisymmetric. They are given by:

$$\sigma_{ij} = \frac{1}{2} \left(\frac{\partial u^j}{\partial x^i} + \frac{\partial u^i}{\partial x^j} \right) - \frac{1}{3} \theta \delta_{ij}, \quad (2)$$

$$\omega_{ij} = \frac{1}{2} \left(\frac{\partial u^j}{\partial x^i} - \frac{\partial u^i}{\partial x^j} \right). \quad (3)$$

where $\theta = \nabla_{\vec{x}} \cdot \vec{u}$ is the expansion.

Recalling that $\delta = \rho/\bar{\rho} - 1 = (a/R)^3 - 1$ (a is the scale factor and R the radius of the perturbation), and inserting it into Eq. 1, it is easy to check that the evolution equation for δ reduces to the SCM (Fosalba & Gaztañaga 1998; Engineer et al. 2000; Ohta et al. 2003)

$$\frac{d^2 R}{dt^2} = 4\pi G\bar{\rho}R - 1/3(\sigma^2 - \omega^2)R = -\frac{GM}{R^2} - 1/3(\sigma^2 - \omega^2)R, \quad (4)$$

comparable with the usual expression for the SCM with angular momentum (e.g. Peebles 1993; Nusser 2001; Zukin & Bertschinger 2010):

$$\frac{d^2 R}{dt^2} = -\frac{GM}{R^2} + \frac{L^2}{M^2 R^3} = -\frac{GM}{R^2} + \frac{4}{25}\Omega^2 R, \quad (5)$$

where in the last expression we have used the momentum of inertia of a sphere, $I = 2/5MR^2$.

The previous argument shows that vorticity, ω , is strictly connected to angular velocity, Ω (see also Chernin (1993), for a complete treatment of the interrelation of vorticity and angular momentum in galaxies).

One assumption generally used when solving the SCM equations for the density contrast δ (Eq. 1) is to neglect the shear, σ , and the rotation ω . While the first assumption is correct, since for a sphere the shear tensor vanishes, the rotation term, or angular momentum is not negligible. In fact, if we consider the ratio of the rotational term and the gravitational one in Eq. 5 we get $\frac{L^2}{M^3 R G}$ that

¹ A slightly overdense sphere, embedded in the universe, is a useful non-linear model, as it behaves exactly as a closed sub-universe because of Birkhoff's theorem.

² r_* is the maximum radius of oscillation of a particle

for a spiral galaxy like the Milky Way, with $L \simeq 2.5 \times 10^{74} \text{ g cm}^2 / \text{s}$ (Ryden & Gunn 1987; Catelan & Theuns 1996), and radius 15 kpc is of the order of 0.4, showing, as well known, that the rotation is not negligible in the case of galaxy sized perturbations. The quoted ratio is larger for smaller size perturbations (dwarf galaxies size perturbations) and smaller for larger size perturbations (for clusters of galaxies the ratio is of the order of 10^{-6}). The value of angular momentum, L , or similarly Ω , can be obtained and added to the SCM as described in Del Popolo (2009) or as described previously, assigning an angular momentum $\propto \sqrt{GM(< r_*)}r_*$ at turn-around (e.g. White & Zaritsky 1992; Sikivie et al. 1997; Nusser 2001).

As previously stressed, the non-trivial role of angular momentum in the SCM has been pointed out in a noteworthy number of papers studying structure formation in DM dominated universes (see also Del Popolo 2009; Zuckin & Bertschinger 2010; Cupani et al. 2011). In a previous letter, Del Popolo et al. (2012) studied the effect of the term $\sigma^2 - \omega^2$ on the SCM parameters (δ_c and Δ_V) for the Einstein-de Sitter (EdS) and Λ CDM models, but it has never taken into consideration in the SCM in DE cosmologies.

In the present paper, we shall study how the typical parameters of the SCM (in Universes dominated by DE), namely the linear density threshold for collapse δ_c and the virial overdensity Δ_V , are changed by a non-zero σ and ω terms. In fact, any extension of the SCM should take into account the effects of shear (Engineer et al. 2000; Del Popolo et al. 2012) since shear induces contraction while vorticity induces expansion as expected from a centrifugal effect. We also study how angular momentum and shear influence the cumulative mass function.

The paper is organized as follows. In Sect. 2, we summarize the model used to obtain δ_c and the virial overdensity Δ_V . In Sect. 3, we describe the results, and Sect. 4 is devoted to conclusions.

2 SUMMARY OF THE MODEL

The evolution equations of δ in the non-linear regime has been obtained and used in the framework of the spherical and ellipsoidal collapse, and structure formation by Bernardeau (1994); Padmanabhan (1996); Ohta et al. (2003, 2004); Abramo et al. (2007). As a first step we assume that the fluid satisfies the equation-of-state $P = w\rho c^2$. In addition, we also consider the Neo-newtonian expressions (Lima et al. 1997) for the continuity, the Euler equations, and the relativistic Poisson equation, namely:

$$\frac{\partial \rho}{\partial t} + \nabla_{\vec{r}} \cdot (\rho \vec{v}) + \frac{P}{c^2} \nabla_{\vec{r}} \cdot \vec{v} = 0, \quad (6)$$

$$\frac{\partial \vec{v}}{\partial t} + (\vec{v} \cdot \nabla_{\vec{r}}) \vec{v} + \nabla_{\vec{r}} \Phi = 0, \quad (7)$$

$$\nabla^2 \Phi - 4\pi G \left(\rho + \frac{3P}{c^2} \right) = 0, \quad (8)$$

where \vec{v} is the velocity in three-space, Φ is the Newtonian gravitational potential and \vec{r} is the physical coordinate.

The continuity equation for the mean background density can be written in the form

$$\dot{\bar{\rho}} + 3H \left(\bar{\rho} + \frac{P}{c^2} \right) = 0, \quad (9)$$

where $\bar{\rho} = \frac{3H^2 \Omega_{\text{fluid}}}{8\pi G}$ is the background mass density of all contributions to the cosmic fluid, and Ω_{fluid} is its density parameter.

Using comoving coordinates $\vec{x} = \vec{r}/a$, the perturbations equa-

tions can be written as

$$\dot{\delta} + (1+w)(1+\delta) \nabla_{\vec{x}} \cdot \vec{u} = 0, \quad (10)$$

$$\frac{\partial \vec{u}}{\partial t} + 2H \vec{u} + (\vec{u} \cdot \nabla_{\vec{x}}) \vec{u} + \frac{1}{a^2} \nabla_{\vec{x}} \phi = 0, \quad (11)$$

$$\nabla_{\vec{x}}^2 \phi - 4\pi G(1+3w)a^2 \bar{\rho} \delta = 0. \quad (12)$$

where $H(a)$ is the Hubble function and $\vec{u}(\vec{x}, t)$ is the comoving peculiar velocity. Combining the previous equations, we get the non-linear evolution equation

$$\begin{aligned} \ddot{\delta} + \left(2H - \frac{\dot{w}}{1+w} \right) \dot{\delta} - \frac{4+3w}{3(1+w)} \frac{\dot{\delta}^2}{1+\delta} - \\ 4\pi G \bar{\rho} (1+w)(1+3w) \delta (1+\delta) - \\ (1+w)(1+\delta)(\sigma^2 - \omega^2) = 0. \end{aligned} \quad (13)$$

which is a generalization of Eq. 7 of Abramo et al. (2007) to the case of a non-spherical configuration of a rotating fluid.

In the case of dust ($w = 0$), Eq. 13 reads

$$\begin{aligned} \ddot{\delta} + 2H \dot{\delta} - \frac{4}{3} \frac{\dot{\delta}^2}{1+\delta} - 4\pi G \bar{\rho} \delta (1+\delta) - \\ (1+\delta)(\sigma^2 - \omega^2) = 0. \end{aligned} \quad (14)$$

which is Eq. 41 of Ohta et al. (2003).

In terms of the scale factor, a , the nonlinear equation driven the evolution of the overdensity contrast can be rewritten as:

$$\begin{aligned} \delta'' + \left(\frac{3}{a} + \frac{E'}{E} \right) \delta' - \frac{4}{3} \frac{\delta'^2}{1+\delta} - \frac{3}{2} \frac{\Omega_{m,0}}{a^5 E^2(a)} \delta (1+\delta) - \\ \frac{1}{a^2 H^2(a)} (1+\delta)(\sigma^2 - \omega^2) = 0, \end{aligned} \quad (15)$$

where $\Omega_{m,0}$ is the density parameter of the DM at $a = 1$, $E(a)$ is given by

$$E(a) = \sqrt{\frac{\Omega_{m,0}}{a^3} + \frac{\Omega_{K,0}}{a^2} + \Omega_{Q,0} g(a)}, \quad (16)$$

where $g(a)$ is

$$g(a) = \exp \left(-3 \int_1^a \frac{1+w(a')}{a'} da' \right). \quad (17)$$

Note that in Eq. 15 we corrected a typo present in Eq. 17 of Pace et al. (2010).

In order to calculate the threshold for the collapse δ_c and the virial overdensity, Δ_V , of the SCM, we follow Pace et al. (2010). We look for an initial density contrast such that the δ solving the non-linear equation diverges at the chosen collapse time. Once the initial overdensity is found, we use this value as an initial condition in the linearised equation

$$\delta'' + \left(\frac{3}{a} + \frac{E'}{E} \right) \delta' - \frac{3}{2} \frac{\Omega_{m,0}}{a^5 E^2} \delta = 0, \quad (18)$$

to get δ_c .

The initial conditions to solve the second-order differential equations are δ_i (got as previously described) and the initial rate of evolution, δ'_i is calculated as follows. We assume that at early times the solution is a power law, therefore we can write $\delta_i = B a^n$, where n is in general of the order unity. The velocity is defined as the derivative with respect to the scale factor of the initial overdensity, hence we can write it as $\delta'_i = n \delta_i / a$.

The virial overdensity is obtained, as in Pace et al. (2010), by using the definition $\Delta_V = \log(\delta_{nl} + 1) = \zeta(x/y)^3$, where $x =$

a/a_{ta} is the normalised scale factor and y is the radius of the sphere normalised to its value at the turn-around.

The turn-around scale factor is obtained by solving Eq. 15 and determining the quantity $\log(\delta_{\text{nl}} + 1)/a^3$. The virial overdensity at turn-around ζ , is obtained by integrating Eq. 15 up to a_{ta} and add the result to unity.

In order to integrate Eq. 15, we should explicit the $\sigma^2 - \omega^2$ term. The calculation of the term $\sigma^2 - \omega^2$ is explained in detail in Del Popolo et al. (2012). Here we simply summarize how we evaluated it.

We first define with α the dimensionless ratio between the rotational and the gravitational term in Eq. (5):

$$\alpha = \frac{L^2}{M^3 R G}, \quad (19)$$

having different values for different scales, as already reported.

We may calculate the same ratio between the gravitational and the extra term appearing in Eq. 15 thereby writing the term extending the standard SCM as

$$\frac{\sigma^2 - \omega^2}{H_0^2} = -\frac{3}{2} \frac{\alpha \Omega_{\text{m},0}}{a^3} \delta, \quad (20)$$

as recently discussed in the literature (Del Popolo et al. 2012).

In order to obtain a value for δ_c similar to the one obtained by Sheth & Tormen (1999), we set $\alpha = 0.05$ for galactic masses ($M \approx 10^{11} M_\odot$) corresponding to a rotational velocity of $v_r \approx 250 \text{ km/s}$ and scaled it linearly towards higher masses and low velocities by assuming a rotational velocity of nearly 10 km/s for galaxy cluster size objects ($M \approx 10^{15} M_\odot$).

Given the above ansatz, the nonlinear equation that has to be satisfied by the overdensity contrast δ for a large class of noninteracting dark energy models reads:

$$\delta'' + \left(\frac{3}{a} + \frac{E'}{E} \right) \delta' - \frac{4}{3} \frac{\delta'^2}{1 + \delta} - \frac{3}{2} \frac{\Omega_{\text{m},0}(1 - \alpha)}{a^5 E^2(a)} \delta(1 + \delta) = 0. \quad (21)$$

It should be remarked that the DE models used are the same of Pace et al. (2010), namely the Λ CDM model, the quintessence models, phantom models and topological defects, and the Chaplygin gas and Casimir effect. We refer to Pace et al. (2010) for more details on the models used.

3 RESULTS

In this section we present results for the two main quantities derived in the framework of the SCM, in particular the linear overdensity parameter δ_c and the virial overdensity Δ_V . We assume as reference model the Λ CDM model, with the following cosmological parameters: $\Omega_{\text{m}} = 0.274$, $\Omega_{\text{de}} = 0.726$ and $h = 0.7$.

First of all, in Fig. 1, we show the linear overdensity parameter δ_c for the EdS model (upper panel) and Λ CDM model (lower panel) as a function of the redshift and of the mass of the collapsing object. Even if a projection of this plot was shown in Del Popolo et al. (2012), we here propose the surface spanned by δ_c to briefly summarize how this quantity depends on the mass and on the redshift.

An important result that it is worth to notice, is the time behaviour of δ_c . We observe that the contribution of the term $\sigma^2 - \omega^2$ is maximum at $z = 0$ and it decreases with increasing redshift till δ_c reaches an approximately constant value, generally higher or equal to the value for the standard SCM, according to the mass range considered. This is expected when we compare the nonlinear term with the gravitational term. The net result is that of giving

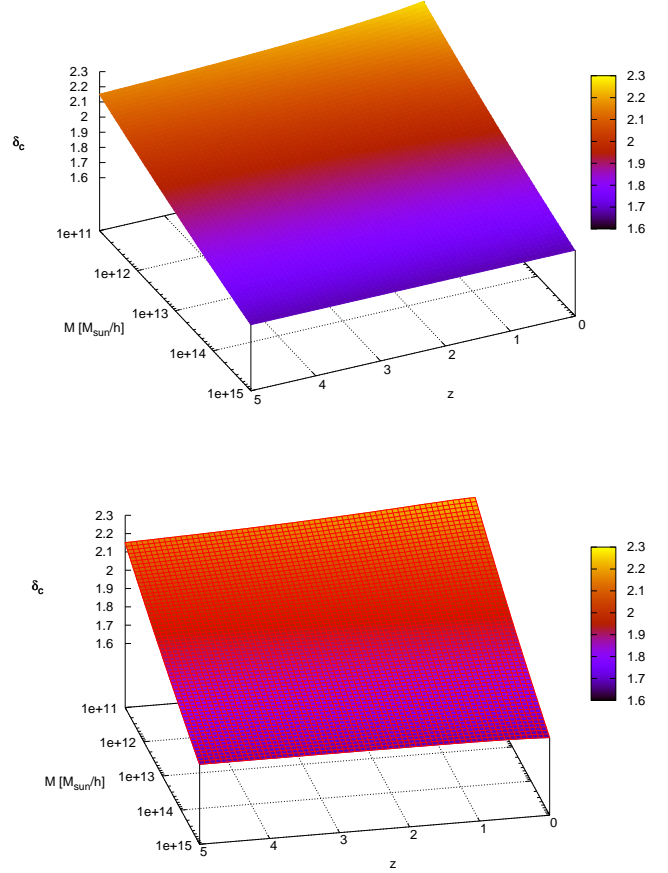


Figure 1. Linear overdensity parameter δ_c as a function of mass and redshift for the EdS model (upper panel) and Λ CDM model (lower panel).

as source term a model with an effective matter density $(1 - \alpha)$ times smaller than the real matter density Ω_{m} (only in the non-linear regime though). This can be interpreted as an additional term counteracting the collapse even at high redshifts, making therefore δ_c higher than the standard value.

In Fig. 2 instead we present results for the different dark energy models considered in this work. On the left panel we show results for the linear overdensity parameter δ_c while on the right panel we show the expected values for the virial overdensity Δ_V . Because of the consideration expressed above regarding the EdS model, we will consider as reference the standard Λ CDM model (with $\alpha = 0$) and to maximize the effect of the non linear term, all the figures show results for galactic masses ($M \approx 10^{11} M_\odot/h$).

For the first class of models (INV1, INV2, 2EXP, AS, CNR, CPL, SUGRA) we see that the models are in general very similar to each other and they slightly differ from each other, with differences at most of the order of 4.5% for the AS model. The INV1, CNR and 2EXP models are basically indistinguishable from the Λ CDM model. We interpret this result as due to the equation of state of the models considered. As shown in Pace et al. (2010), the INV1 model has an equation of state basically constant over the whole cosmic history, but its present value is quite different from all the other models, being $w_0 \approx -0.4$, while for all the other models is $-1 \leq w_0 \leq -0.8$.

Comparing our present results with the ones of the upper left panel in Fig. 4 of Pace et al. (2010), we see that the behaviour of the

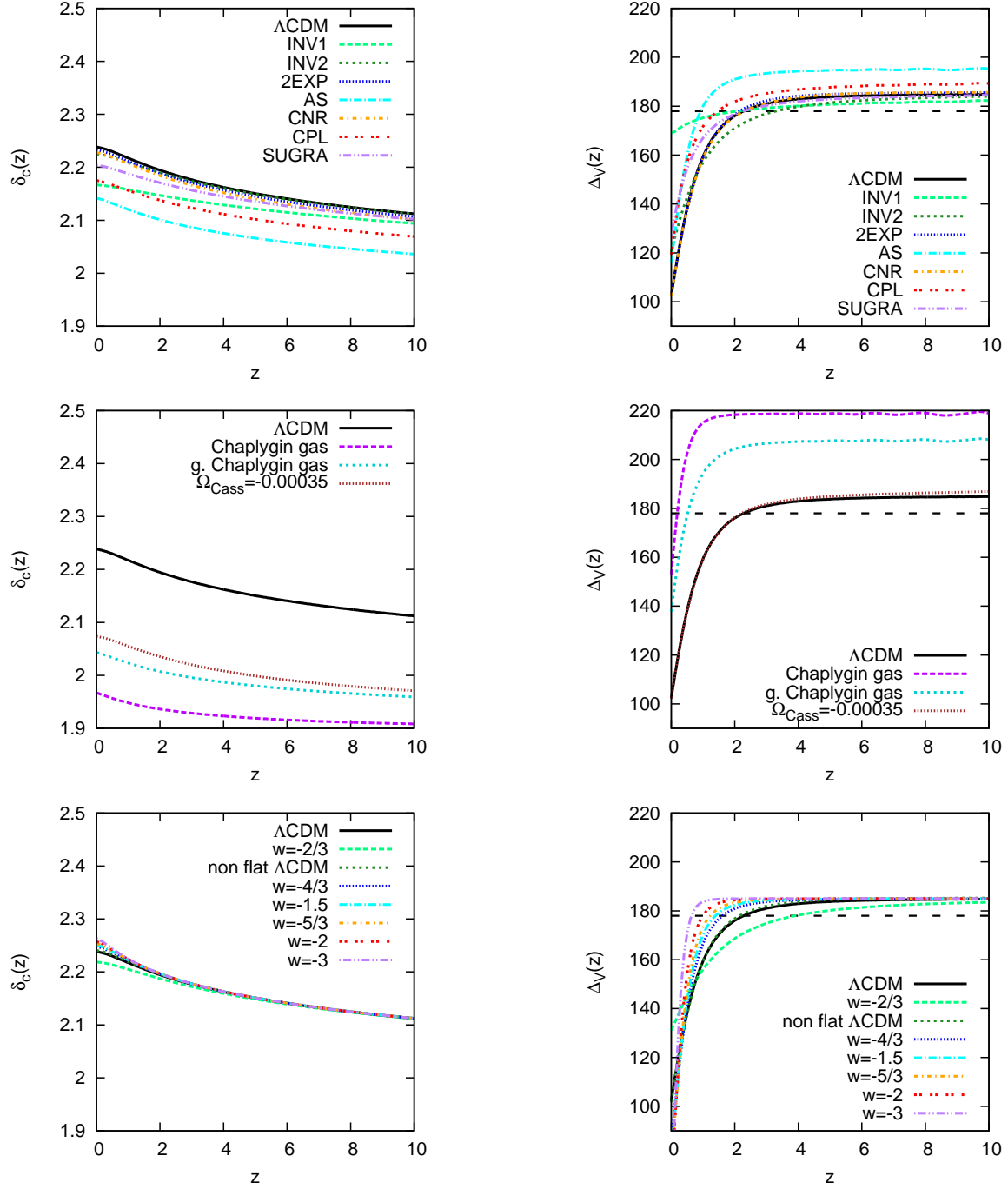


Figure 2. The left panels show the time evolution of the linear overdensity $\delta_c(z)$, the right panels the time evolution for the virial overdensity $\Delta_V(z)$ for the different classes of models. In all panels, the Λ CDM solution (black solid curve) is the reference model. All the curves assume a galactic mass for the collapsing sphere. The upper panels present the quintessence models: the INV1 (INV2) model is shown with the light-green dashed (dark-green short-dashed) curve, the 2EXP model with the blue dotted curve, the AS model with the cyan dot-dashed curve, the CPL (CNR) model with the red dot-dotted (orange dot-short-dashed) curve and finally the SUGRA model with the violet dot-dot-dashed curve. The middle panels show the Casimir effect (brown dotted curve) and the (generalized) Chaplygin gas with the (turquoise short-dashed) magenta dashed curve. Finally the lower panels report the solution for the models with constant equation-of-state parameter: the dark-green short-dashed curve stands for the non-flat Λ CDM model, the light-green dashed curve for the model with $w = -2/3$, the blue dotted curve represents the model with $w = -4/3$, the cyan dot-dashed curve the model with $w = -1.5$, the orange dot-short-dashed curve the model with $w = -5/3$, the red dot-dotted curve the model with $w = -2$ and finally the violet dot-dot-dashed curve shows the model with $w = -3$.

models is very similar. The inclusion of the non-linear term just changes the values of the linear overdensity parameter, but not the respective ratios with the Λ CDM model.

For the second group of models (Casimir and (generalized) Chaplygin gas) we obtain very different results from Pace et al. (2010). While there only the generalised Chaplygin gas was substantially different from the Λ CDM model, now all the models here considered differ much from the reference model. This shows how the non-linear additional term is very sensitive to the equation of state considered. Moreover, none of the models recovers the extended Λ CDM model at high redshifts.

The bottom panel in the left column is devoted to the phantom models ($w < -1$) and to a non-flat Λ CDM model. All the models present very similar results and small differences appear at small redshifts ($z \lesssim 1$), and for redshifts $z \gtrsim 2$, all the models are identical. Models differing most at $z \approx 0$ are the models with $w = -2/3$ and $w = -3$ having values for δ_c respectively lower and higher than the Λ CDM model. This is in agreement with results of Pace et al. (2010), showing once again that a super-negative equation-of-state affects only slightly the structure formation process. In particular, the more negative it is, the higher is the linear overdensity parameter. We also notice that a small amount of curvature, does not influence our results significantly.

Comparing these results, with the results from Fig. 4 in Pace et al. (2010), we can appreciate the interplay between the term $\sigma^2 - \omega^2$ and a dynamical dark energy equation of state.

All the models studied with a time-varying dark energy equation-of-state parameter show that the collapse, even if retarded by the inclusion of the shear and rotation, is easier as compared with the Λ CDM model. In this case, with easier we mean that the values for the extended $\delta_c(z)$ are smaller than for the reference model. This is expected and it has the same explanation as for the usual case. Since at early times the amount of dark energy is higher, we need structures to grow faster in order to observe cosmic structures today. This is plausible, since the linear overdensity parameter represents the time evolution of the initial overdensity, whose evolution is dictated by the growth rate that is described by the same differential equation. In other words, since at early times the amount of dark energy is higher, we need lower values of δ_c to have objects collapsing. This is analogous to the case of the linear growth factor, since the equation to be solved is the same.

Opposite is instead the behaviour for the phantom models, in which case we notice that with a more negative equation of state, the collapse is retarded more severely. This is in agreement with Fig. 4 of Pace et al. (2010), where phantom models had an higher δ_c : since the expansion goes so fast, the collapse is strongly suppressed and with respect to the reference models, higher and higher initial overdensities are required in order to have collapsed objects today.

On the right panels, we show results for the quantity Δ_V . Also in this case we limit ourselves to galactic masses. We notice that for the quintessence models in general the virial overdensity shows higher values than for the extended Λ CDM model, except for the INV2 model. This is opposite to what found for the standard case, where all the models had smaller values than the Λ CDM model. Also in this case none of the models approximates the extended Λ CDM model at high redshifts. This is not the result of the additional non-linear term only, but also of the influence of the dark energy equation of state, consistently with results from Pace et al. (2010).

For the phantom models, results are very similar to the usual case. Virial overdensity parameter is higher than the extended Λ CDM one if $w < -1$ and lower for the model with $w = -2/3$,

Table 1. Table with the power spectrum normalization for the different dark energy models (K is the curvature parameter).

Model	σ_8
Λ CDM, $K=0$	0.776
Λ CDM, $K \neq 0$	0.793
INV1	0.428
INV2	0.707
2EXP	0.739
AS	0.319
CNR	0.732
CPL	0.444
SUGRA	0.578
Chaplygin gas	0.066
g. Chaplygin gas	0.133
Casimir	0.420
Phantom ($w = -2/3$)	0.674
Phantom ($w = -4/3$)	0.834
Phantom ($w = -1.5$)	0.854
Phantom ($w = -5/3$)	0.870
Phantom ($w = -2$)	0.894
Phantom ($w = -3$)	0.936

in agreement with the linear overdensity parameter. As shown in Pace et al. (2010), at higher redshifts, all the phantom models reduce to the Λ CDM model.

Differences in the linear overdensity parameter reflect in the differential mass function. In this work we decide to use the parametric form by Sheth & Tormen (1999); Sheth et al. (2001); Sheth & Tormen (2002). We consider three different redshifts, namely $z = 0, 0.5, 1$.

At this point, it is worth noticing that in the first paper of Sheth & Tormen (1999) the mass function was calculated as a fit to numerical simulations. Later on, Sheth et al. (2001) and Sheth & Tormen (2002) showed that the effects of non-sphericity (shear and tides) introduce a mass dependence in the collapse threshold (see Eq. 4 in Sheth et al. (2001) and following discussion). By using this threshold as the barrier in the excursion set approach one gets a mass function in good agreement with simulations (see Eq. 5 and the discussion in the last part of Sect. 2.2. of Sheth et al. (2001), and moreover Sheth & Tormen (2002)).

For the Λ CDM model we choose as power spectrum normalization the value $\sigma_8 = 0.776$. Since we want that perturbations at the CMB epoch are the same for all the models, we normalize the dark energy model according to the formula

$$\sigma_{8,DE} = \sigma_{8,\Lambda\text{CDM}} \frac{D_{+, \Lambda\text{CDM}}(a_{\text{CMB}})}{D_{+, DE}(a_{\text{CMB}})}, \quad (22)$$

where $D_+(a_{\text{CMB}})$ is the growth factor at the CMB epoch.

In Table 1, we display the different normalizations used for the models considered in this work (K is the curvature parameter).

In Fig. 3 we compare the differential mass function for the Λ CDM model in the standard and in the extended SCM.

Analysing the three curves, we can appreciate the effect of the term $\sigma^2 - \omega^2$ on the mass function. On small masses, the mass function is largely independent of the cosmological model, but it depends strongly on δ_c . Since in the extended SCM this is higher, we observe an increase in the number of objects at galactic scale at $z = 0$, to decrease at higher redshifts where the contribution of the non-linear term decreases. We observe a general decrement in the

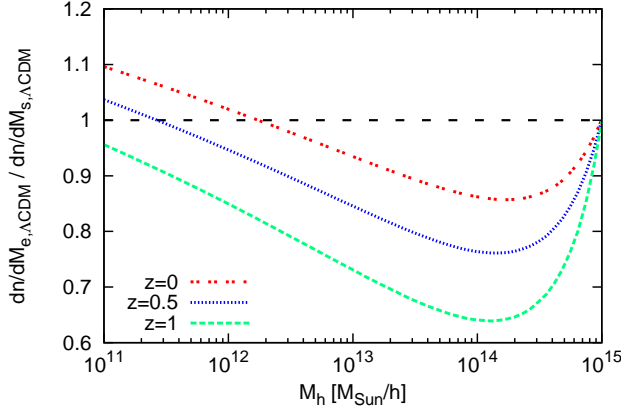


Figure 3. Ratio between the differential mass function of the extended and standard Λ CDM model. The curves represent three different redshifts: $z = 0$ (dotted red curve), $z = 0.5$ (short-dashed blue curve), $z = 1$ (dashed green curve).

number of objects at high masses (up to $M \approx 10^{14} M_\odot/h$) to increase again to unity for masses of the order of $10^{15} M_\odot/h$. This is explained by the fact that at such masses, the linear overdensity parameter are practically the same, therefore the mass function must not change.

In this concern, it should be recalled that shear and rotation have the maximum effect on δ_c , at galactic scale (see Fig. 1). However, in the calculation of the ratio between the differential mass functions (Fig. 3), beside δ_c we need to take into account the factor $\sigma(M)$, the r.m.s. of mass overdensity. Now, recalling the Sheth & Tormen multiplicity function

$$f_{ST} = A \sqrt{\frac{2a}{\pi}} \left[1 + \left(\frac{\sigma(M)^2}{\delta_c^2 a} \right)^p \right] \frac{\delta_c}{\sigma(M)} e^{-\frac{a\delta_c^2}{2\sigma(M)^2}}, \quad (23)$$

with $A = 0.3222$, $a = 0.707$, and $p = 0.3$, we have that at galactic scale the dominant term in Eq. 23 is the term $\frac{\delta_c}{\sigma}$, consequently the ratio $f_{ST,extended}/f_{ST,\Lambda CDM} \simeq \delta_{c,extended}/\delta_{c,\Lambda CDM}$. At larger masses, the effect of rotation and shear diminishes with the consequence that $\delta_{c,extended} \simeq \delta_{c,\Lambda CDM}$ and that the $\sigma(M)$ term is fixing the value of the $f_{ST,extended}/f_{ST,\Lambda CDM}$ ratio.

At this point it is necessary a deeper discussion of the results shown in Fig. 3. The ST mass function generalises the Press & Schechter (PS) (Press & Schechter 1974) mass function to include the effects of shear and tidal forces with respect to the simpler spherical collapse model. In doing so it is necessary to consider the ellipsoidal collapse model and the corresponding linear overdensity parameter δ_{ec} . Differently from the spherical collapse model, now δ_{ec} is not only a function of time, but of mass too and the relation between δ_{ec} and δ_c (δ_{sc} in Sheth et al. (2001)) is given by Eq. 4 in Sheth et al. (2001). The moving barrier for the random walk is now set equal to $\delta_{ec}(M, z)$ and a good approximation to it is then given by their Eq. 5. The ST mass function fits quite well the results of N-body simulations, but as shown in Fig. 3, for masses $M \approx 10^{14} M_\odot/h$ our predictions, including rotation on top of the ellipsoidal collapse, predict approximately 40% less objects at $z = 1$ than the standard Λ CDM model. This would be easily checked with a big enough spanned volume. Moreover one could identify ellipticity and rotation if halos acquire angular momentum by misalignment with the surrounding tidal field. Following this line of thought one could further use the $\delta_c(M, z)$ predicted by the extended spherical collapse model as the correct moving barrier.

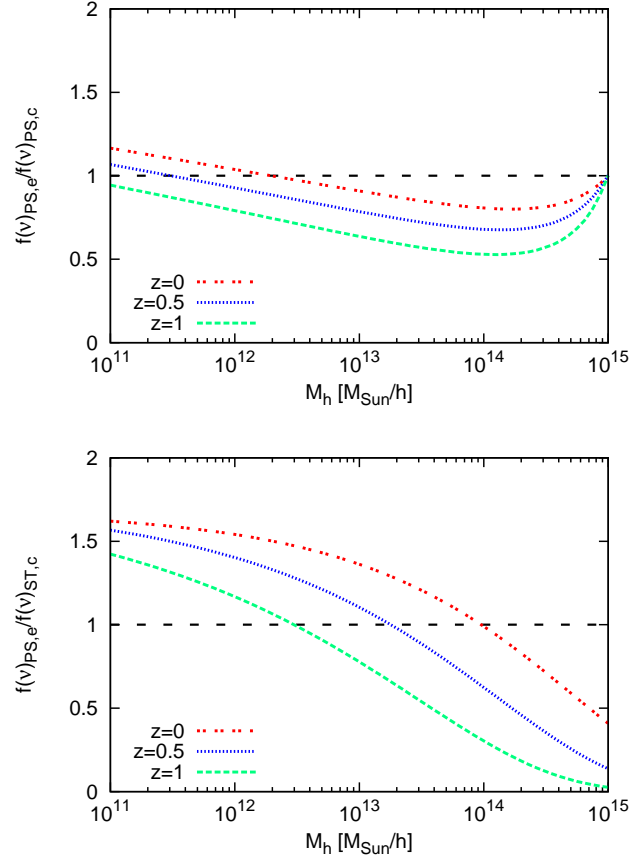


Figure 4. Ratio between the PS multiplicity function evaluated with $\delta_{c,extended}$ and $\delta_{c,\Lambda CDM}$ (upper panel) and ratio between the PS multiplicity function with $\delta_{c,extended}$ and the ST multiplicity function with $\delta_{c,\Lambda CDM}$. Line styles and colours are as in Fig. 3.

Therefore by direct comparison of expressions (2), (4) and (5) in Sheth et al. (2001) we substitute $\delta_{c,extended}$ directly into their expression (2) (equivalent to the PS multiplicity function). Results are shown in Fig. 4 for the three redshifts of Fig. 3.

In the upper panel we show the ratio of the PS multiplicity function evaluated with the $\delta_{c,extended}$ and $\delta_{c,\Lambda CDM}$ linear overdensity parameters while in the lower panel we compute the ratio of the PS multiplicity function evaluated with the $\delta_{c,extended}$ linear overdensity parameter with the ST multiplicity function evaluated with the $\delta_{c,\Lambda CDM}$ linear overdensity parameter. As it is evident, when we compute the ratio using the same multiplicity function, we obtain a very similar behaviour as in Fig. 3, even if quantitatively slightly different. When we instead identify rotation with ellipticity and use directly the PS multiplicity function and compare it with the ST multiplicity function, we observe a totally different behavior. This can be explained not only in terms of different overdensity parameters, but also remembering that the PS mass function predicts more (less) objects at low (high) masses with respect to the ST parametrization. Our results also show that if we want to reproduce the results of the ST mass function using the extended spherical collapse model, we need to modify the moving barrier and find a new parametrization for the multiplicity function. This goes beyond the purpose of this work, therefore, taking into account these caveats we will assume the ST mass function as the correct one.

In Fig. 5 we show the ratios, at the three different redshifts

considered, between the different dark energy models here considered and the extended Λ CDM model, where the term $\sigma^2 - \omega^2$ is included.

As we can notice, the (generalised) Chaplygin gas shows a huge suppression of structures at all redshifts, making therefore this model ruled out in the extended SCM. All quintessence models have a lack of high mass objects. While this is not severe at all for the INV2, 2EXP and CNR model, all the others have a suppression of several orders of magnitude, increasing with the increase on the redshift. The most suppressed model is the AS model, that shows also the most different δ_c from the extended Λ CDM model.

Regarding the phantom models, differences are at most of a factor of 4-5. While the model with $w = -2/3$ shows a decrease in structures, the phantom models show an increase. Differences are significant in general only for high masses $M \gtrsim 10^{14} M_\odot/h$ while for the model with $w = -2/3$, they are evident already at $M \approx 10^{13}$ for $z = 1$.

We also notice that a small amount of curvature has a very little effect on the number of objects, as differences are of the order of few percent even for cluster scales.

Our results can be easily interpreted in terms of the different matter power spectrum normalizations. The Chaplygin gas has an extremely low normalization ($\sigma_8 = 0.066$) making therefore very unlucky that structures could form in such a universe. Phantom models instead show an higher normalization, making therefore easier to have high mass objects. Moreover one has to take into account that now the linear overdensity parameter δ_c is modified and very strong differences will reflect in the differential mass function (see for example Fig. 2).

A direct comparison between the results in this work and the ones described in Pace et al. (2010) cannot be made for several reasons. In particular, the power spectra here were normalised in order to have the same amplitude of fluctuations at the CMB epoch while in Pace et al. (2010) a different normalisation was adopted. There the power spectrum was normalised in order to have nearly the same mass function at $z = 0$. This implies that effects of dark energy will be important only at high redshifts while in our case we see substantial differences already at low redshifts as expected. In addition, here we just limit ourselves to the study of the differential mass function and we do not investigate the cumulative number of halos. This is because we do not want to have our results affected by volume effects. Note also that due to the choice of normalization in Pace et al. (2010), the quintessence models will predict more objects than the Λ CDM at high redshifts (not shown here).

4 CONCLUSIONS

In this work, we study the impact of the term $\sigma^2 - \omega^2$ on the spherical collapse parameters, namely the linear overdensity parameter δ_c and the virial overdensity parameter Δ_V and how this reflects on the number of objects via the mass function formalism for a broad class of dark energy models, already studied in the spherical limit, by Pace et al. (2010).

We assume that only the dark matter component is clustering and that dark energy is only at the background level, therefore affecting only the time evolution of the Universe. Doing this, we implicitly assumed that eventual perturbations in the dark energy component can be neglected.

We showed that the non-linear term considered opposes to the collapse and this is reflected by higher values of the linear overdensity parameter with respect to the spherical case. Modifications are

quite substantial, of the order also of 40% for the Λ CDM model. In general the effect of dark energy is to lower the value of δ_c with respect to the Λ CDM model and we see that this is also the case also in the extended SCM. Despite the values of the linear overdensity parameter are higher now than in the non-rotating case, we see that in general dark energy still lowers its value. This is the case only if $w > -1$, while for phantom models the super-negative equation of state slows down the collapse.

In order to appreciate the interplay between the different dark energy equation-of-state parameter and the power spectrum normalization, it is interesting to compare models having approximately the same power spectrum normalization. For example, this is the case for the models INV1, CPL and Casimir (see Table 1 for the exact values). Having very similar power spectra normalizations, from Fig. 5 we see that the ratio with the Λ CDM mass function gives in general very similar results. Models INV1 and CPL are very similar to each other and in general similar to the Casimir model. Differences between these models can be seen more clearly in the evolution of δ_c in Fig. 2. This shows that often differences in the models are hidden by the power spectrum normalization. In general, taking into account this caveat, for other models differences in the differential mass function are due to the influence of the dark energy component (see also comments at the end of Sect. 3).

As expected, such differences reflect in the number of objects. Since with respect to the standard case the only quantity to be changed is δ_c , we can easily study the impact of a rotation term on structure formation. We show this in Fig. 5. The term $\sigma^2 - \omega^2$ suppresses, as expected, the high mass tail of the mass function, since rare events are more sensitive to the background cosmology and to the collapse process. In general low masses objects are not severely affected by rotation, but a noteworthy counterexample is given by the (generalized) Chaplygin gas and AS model where we observe a suppression in the number of objects already of several orders of magnitude for galactic masses.

We conclude therefore that the term $\sigma^2 - \omega^2$ has a strong impact on structure formation and that it is worth to investigate different parametrizations for the additional term.

ACKNOWLEDGEMENTS

The authors would like to thank the referee Y. Ascasibar for the valuable comments that improved our manuscript. ADP is partially supported by a visiting research fellowship from FAPESP (grant 2011/20688-1), and wishes also to thank the Astronomy Department of São Paulo University for the facilities and hospitality. FP is supported by STFC grant ST/H002774/1, and JASL is also partially supported by CNPq and FAPESP under grants 304792/2003-9 and 04/13668-0.

References

- Abramo L. R., Batista R. C., Liberato L., Rosenfeld R., 2007, *Journal of Cosmology and Astro-Particle Physics*, 11, 12
- Alcaniz J. S., Lima J. A. S., Cunha J. V., 2003, *MNRAS* 340, L39
- Allen S. W., Rapetti D. A., Schmidt R. W., Ebeling H., Morris R. G., Fabian A. C., 2008, *MNRAS*, 383, 879
- Allen S. W., Schmidt R. W., Ebeling H., Fabian A. C., van Speybroeck L., 2004, *MNRAS*, 353, 457
- Amendola L., Gannouji R., Polarski D., Tsujikawa S., 2007, *Phys. Rev. D*, 75, 083504

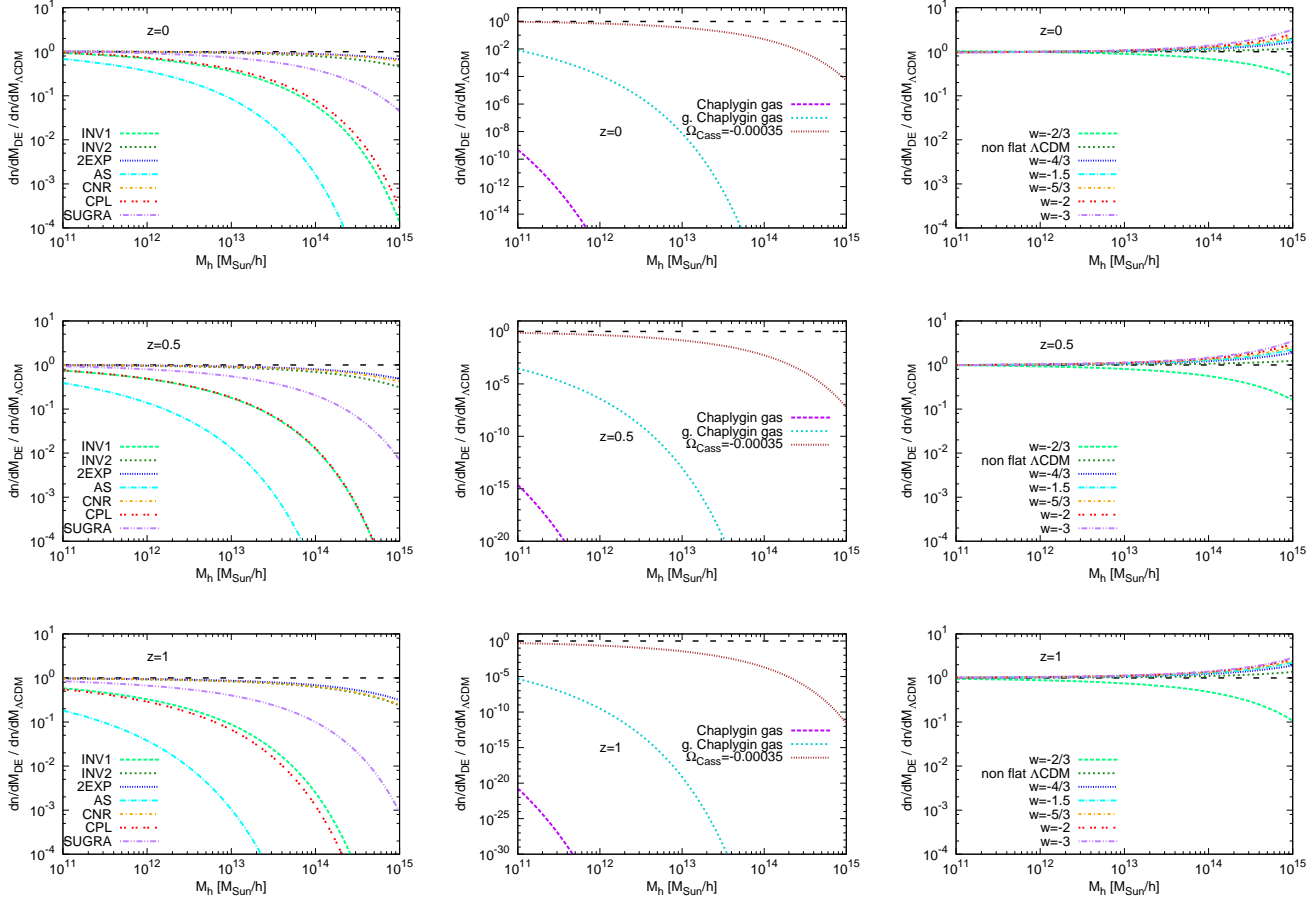


Figure 5. Differential mass function for the dark energy models considered in this work in the extended SCM for different redshifts: $z = 0$ (upper panels), $z = 0.5$ (middle panels), $z = 1$ (lower panels). Panels on the left (right) show the quintessence (phantom and non-flat Λ CDM) models, the central panels show the models described by a (generalised) Chaplygin gas and by the Casimir effect. We refer to Fig. 2 for line-styles and colours.

Ascasibar Y., Yepes G., Gottlöber S., Müller V., 2004, MNRAS, 352, 1109
 Astier P., Guy J., Regnault N., Pain R., Aubourg E., Balam D., Basa S., Carlberg R. G., Fabbro S., Fouchez D., et al. 2006, A&A, 447, 31
 Avila-Reese V., Firmani C., Hernández X., 1998, ApJ, 505, 37
 Bardeen J. M., Bond J. R., Kaiser N., Szalay A. S., 1986, ApJ, 304, 15
 Basilakos S., Plionis M., Lima J. A. S. 2010, Phys. Rev. D, 82, 083517
 Basilakos S., Plionis M., Solà J., 2010, Phys. Rev. D, 82, 083512
 Bengochea G. R., Ferraro R., 2009, Phys. Rev. D, 79, 124019
 Bernardreau F., 1994, ApJ, 433, 1
 Bertschinger E., 1985, ApJS, 58, 39
 Catelan P., Theuns T., 1996, MNRAS, 282, 436
 Chernin A. D., 1993, A&A, 267, 315
 Cole S., Percival W. J., Peacock J. A., et al. 2005, MNRAS, 362, 505
 Creminelli P., D'Amico G., Noreña J., Senatore L., Vernizzi F., 2010, JCAP, 3, 27
 Cupani G., Mezzetti M., Mardirossian F., 2011, MNRAS, 417, 2554
 Deffayet C., 2001, Physics Letters B, 502, 199
 Del Popolo A., 2009, ApJ, 698, 2093
 Del Popolo A., Pace F., Lima J. A. S., 2012, ArXiv e-prints

Dotter A., Sarajedini A., Anderson J., 2011, Astrophys. J. 738, 1
 Eisenstein D. J., Zehavi I., Hogg D. W., Scoccimarro R., Blanton M. R., Nichol R. C., Scranton R., Seo H.-J., Tegmark M., Zheng Z., et al. 2005, ApJ, 633, 560
 Engineer S., Kanekar N., Padmanabhan T., 2000, MNRAS, 314, 279
 Fillmore J. A., Goldreich P., 1984, ApJ, 281, 1
 A., Alcaniz J. S., Lima J. A. S., 2005, MNRAS, 362, 1295
 Fosalba P., Gaztañaga E., 1998, MNRAS, 301, 503
 Gunn J. E., Gott III J. R., 1972, ApJ, 176, 1
 Gurevich A. V., Zybin K. P., 1988a, Zhurnal Eksperimental noi i Teoreticheskoi Fiziki, 94, 3
 Gurevich A. V., Zybin K. P., 1988b, Zhurnal Eksperimental noi i Teoreticheskoi Fiziki, 94, 5
 Guth A. H., Pi S.-Y., 1982, Physical Review Letters, 49, 1110
 Haiman Z., Mohr J. J., Holder G. P., 2001, ApJ, 553, 545
 Hawking S. W., 1982, Physics Letters B, 115, 295
 Hiotelis N., 2002, A&A, 382, 84
 Ho S., Hirata C., Padmanabhan N., Seljak U., Bahcall N., 2008, Phys. Rev. D, 78, 043519
 Hoekstra H., Mellier Y., van Waerbeke L., Semboloni E., Fu L., Hudson M. J., Parker L. C., Tereno I., Benabed K., 2006, ApJ, 647, 116
 Hoffman Y., Shaham J., 1985, ApJ, 297, 16
 Hoffman, Y., 1986, ApJ 308, 493

- Hoffman, Y., 1989, *ApJ* 340, 69
- Jarvis M., Jain B., Bernstein G., Dolney D., 2006, *ApJ*, 644, 71
- Knop R. A., Aldering G., Amanullah R., Astier P., Blanc G., Burns M. S., Conley A., Deustua S. E., Doi M., Ellis R., et al. 2003, *ApJ*, 598, 102
- Kolb E. W., Matarrese S., Riotto A., 2006, *New Journal of Physics*, 8, 322
- Komatsu E., Smith K. M., Dunkley J., et al. 2011, *ApJS*, 192, 18
- Krauss L. M., Chaboyer B., 2003, *Science*, 299, 65
- Larson D., Dunkley J., Hinshaw G., Komatsu E., Nolte M. R., Bennett C. L., Gold B., Halpern M., Hill R. S., et al. 2011, *ApJS*, 192, 16
- Le Delliou M., Henriksen R. N., 2003, *A&A*, 408, 27
- Lima J. A. S., Zanchin V., Brandenberger R. H., 1997, *MNRAS* 291, L1
- Mota D. F., van de Bruck C., 2004, *A&A*, 421, 71
- Nusser A., 2001, *MNRAS*, 325, 1397
- Ohta Y., Kayo I., Taruya A., 2003, *ApJ*, 589, 1
- Ohta Y., Kayo I., Taruya A., 2004, *ApJ*, 608, 647
- Pace F., Waizmann J.-C., Bartelmann M., 2010, *MNRAS*, 406, 1865
- Padmanabhan T., 1996, *Cosmology and Astrophysics through Problems*
- Peebles P. J. E., 1993, *Principles of physical cosmology*
- Percival W. J., Reid B. A., Eisenstein D. J., et al. 2010, *MNRAS*, 401, 2148
- Perlmutter S., Aldering G., Goldhaber G., et al. 1999, *ApJ*, 517, 565
- Press, W. H. and Schechter, P., 1974, *ApJ*, 187, 425
- Riess A. G., Filippenko A. V., Challis P., et al. 1998, *AJ*, 116, 1009
- Riess A. G., Strolger L.-G., Tonry J., Casertano S., Ferguson H. C., et al. 2004, *ApJ*, 607, 665
- Ryden B. S., Gunn J. E., 1987, *ApJ*, 318, 15
- Sheth R. K., Mo H. J., Tormen G., 2001, *MNRAS*, 323, 1
- Sheth R. K., Tormen G., 1999, *MNRAS*, 308, 119
- Sheth R. K., Tormen G., 2002, *MNRAS*, 329, 61
- Sikivie P., Tkachev I. I., Wang Y., 1997, *Phys. Rev. D*, 56, 1863
- Starobinsky A. A., 1982, *Physics Letters B*, 117, 175
- Subramanian K., Cen R., Ostriker J. P., 2000, *ApJ*, 538, 528
- Tegmark M., Blanton M. R., Strauss M. A., Hoyle F., Schlegel D., Scoccimarro R., Vogeley M. S., Weinberg D. H., Zehavi I., Berlind A., et al. 2004, *ApJ*, 606, 702
- Tegmark M., Strauss M. A., Blanton M. R., Abazajian K., Dodelson S., Sandvik H., Wang X., Weinberg D. H., Zehavi I., Bahcall N. A., et al. 2004, *Phys. Rev. D*, 69, 103501
- Tonry J. L., Schmidt B. P., Barris B., Candia P., Challis P., Clocchiatti A., Coil A. L., Filippenko A. V., Garnavich P., Hogan C., et al. 2003, *ApJ*, 594, 1
- White S. D. M., Zaritsky D., 1992, *ApJ*, 394, 1
- Williams L. L. R., Babul A., Dalcanton J. J., 2004, *ApJ*, 604, 18
- Zaroubi, S., Hoffman, Y., 1993, *ApJ* 416, 410
- Zukin P., Bertschinger E., 2010, in *APS Meeting Abstracts A Generalized Secondary Infall Model*. p. 13003